

Articles

Understanding the Behavior of Halogens as Hydrogen Bond Acceptors

Lee Brammer,^{*,†} Eric A. Bruton,[†] and Paul Sherwood[‡]

Department of Chemistry and Biochemistry, University of Missouri—St. Louis, 8001 Natural Bridge Road, St. Louis, Missouri 63121-4499, and Computational Science and Engineering Department, CLRC Daresbury Laboratory, Daresbury, Warrington WA4 4AD, U.K.

Received May 3, 2001

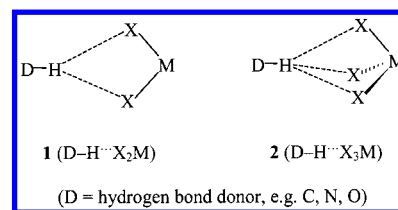
ABSTRACT: The similarities and differences between the behavior of carbon-bound and terminal metal-bound halogens and halide ions as potential hydrogen bond acceptors has been extensively investigated through examination of many thousands of interactions present in crystal structures. Halogens in each of these environments are found to engage in hydrogen bonding, and geometric preferences for these interactions have been established. Notably, typical $\text{H}\cdots\text{X}-\text{M}$ angles are markedly different for $\text{X} = \text{F}$ than for $\text{X} = \text{Cl}, \text{Br}, \text{I}$. Furthermore, there are significant parallels between the behavior of moderately strong hydrogen bond acceptors $\text{X}-\text{M}$ and the much weaker acceptors $\text{X}-\text{C}$. The underlying reasons for the observed geometric preferences have been established by ab initio molecular orbital calculations using suitable model systems. The results are presented within the context of their potential applications in crystal engineering and supramolecular chemistry, including relevance to nucleation in halogenated solvents. The broader implications of the results in areas such as halocarbon coordination chemistry, binary metal halide solid-state chemistry, and the study of weakly coordinating anions are also discussed.

Introduction

The hydrogen bond acceptor capability of halogens has attracted attention on a number of fronts. Halide ligands ($\text{M}-\text{X}$) have been shown to be very good hydrogen bond acceptors,¹ as is the case for halide ions (X^-), while studies of organic halides (principally $\text{C}-\text{F}$ and $\text{C}-\text{Cl}$ groups) have suggested that these are at best very weak hydrogen bond acceptors.^{1a,3}

Hydrogen bonding involving halide ions is, of course, of interest in the context of metabolically important ion channels⁴ and waste remediation involving halide salts. Thus, halide ions have been the target guests in the design of various hydrogen bonding based receptors^{5,6} as well as serving as templates for supramolecular assembly.⁷ Interest in hydrogen bonds involving metal halides ($\text{M}-\text{X}$) lies in materials chemistry,⁸ with suggested applications including magnetic⁹ and thermochromic materials.¹⁰ In organometallic chemistry,^{11–13} interest has centered upon the protonation and protonolysis of metal halides,^{11a} including recent studies in

which bifluoride (HF_2^-)¹² and even HF^{13} have been observed as ligands. The potential for metal halides, particularly fluorides, to serve as receptors for proton donors has also been noted.¹⁴ In the field of crystal engineering, our group and that of Orpen have independently identified so-called supramolecular synthons¹⁵ that utilize the directional properties of metal halides in their formation of hydrogen bonds and can be used to link molecular building blocks. These synthons (**1**^{16,17} and **2**¹⁶) have been applied to the design of



hydrogen-bonded assemblies based upon ammonium and pyridinium salts of perhalometalates. Interest in halocarbons as hydrogen bond acceptors stems in part from the realization that weak hydrogen bonds¹⁸ (and other weak interactions), while not typically dominating the molecular recognition process, nevertheless have an important role to play in influencing, moderating, or

* To whom correspondence should be addressed. Current address: Department of Chemistry, University of Sheffield, Sheffield S3 7HF, U.K. E-mail: lee.brammer@sheffield.ac.uk. Fax: +44 (0)114 273 8673.

[†] University of Missouri—St. Louis.

[‡] CLRC Daresbury Laboratory.

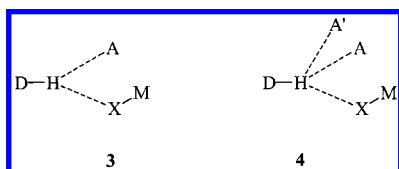
complementing stronger forces. The wide use of halo-carbon solvents in organic and organometallic synthesis and for crystallization purposes makes an understanding of the interactions of halocarbons of broad importance. There has also been specific interest in the hydrogen bond acceptor capability of C–F groups due to the widely used approach of replacing a hydroxy group by fluorine in enzyme substrate analogues.^{3a–e,19}

When considering the use of hydrogen bonds in molecular recognition, either for designing (chemical) receptors or for constructing supramolecular assemblies, it is necessary to have a good understanding of preferred geometries and energetics in order to facilitate an effective design process. In previous communications, we have reported that metal-bound chlorides (M–Cl) are excellent hydrogen bond acceptors, only slightly weaker than chloride ions, while, in contrast, carbon-bound chlorine (C–Cl) is a very poor acceptor.^{1a} We have further identified marked differences in the strength and directionality of metal fluorides as hydrogen bond acceptors relative to their heavier halogen congeners.^{1b}

Here we present a comprehensive study of the geometry of D–H···X–M, D–H···X–C, and D–H···X[–] hydrogen bonds (D = C, N, O; X = F, Cl, Br, I; M = transition metal) based upon a detailed survey of crystallographic data.²⁰ The observed geometries are interpreted with the aid of *ab initio* electronic structure calculations on suitable model compounds. The chemical implications of the findings are discussed in terms of currently accepted ideas on hydrogen bonding and in terms of the relevance to and potential applications in many areas of chemistry.

Experimental Section

CSD Searches, Geometrical Analyses, and Graphical Representation of Data. Geometric data were obtained for D–H···X–M, D–H···X–C, and D–H···X[–] contacts using searches of the Cambridge Structural Database (CSD)^{21,22} (April 1998 release, version 5.16, for X = Cl; April 1999 release, version 5.18, for X = F, Br, I). Only structures that were considered by the CSD to be error-free and not disordered were included. Duplicate structure determinations were inspected individually, and only the most reliable structure was retained. In some cases involving C–H donor groups, further restrictions on structure quality^{22a} were made to ensure that the total number of data (<10 000) could be handled by the CSD data analysis software (VISTA). In all searches, C–H, N–H, and O–H distances were normalized to standard neutron bond lengths, and only those structures containing intermolecular contacts with D–H···X angles of 110° and normalized distance parameter $R_{\text{HX}}^3 = 1.15$ were included in subsequent analyses.^{22b} Normalized distances, $R_{\text{HX}} = d(\text{H}\cdots\text{X})/(r_{\text{H}} + r_{\text{X}})$, were calculated on the basis of van der Waals radii: $r_{\text{H}} = 1.20$, $r_{\text{F}} = 1.47$, $r_{\text{Cl}} = 1.75$, $r_{\text{Br}} = 1.85$, and $r_{\text{I}} = 1.96$.²³ Only terminally bound halogens were considered. Separate searches were conducted first for all hydrogen bonds involving a given donor and acceptor group, and then subsequent searches were used to identify bifurcated (**3**) and trifurcated (**4**) hydrogen bonds for



all donor–acceptor combinations, where A, A' = N, P, As, O, S, Se, F, Cl, Br, I. Cases in which A and/or A' are bonded to

M, as well as those in which they are not, were permitted. On the basis of a comparison of the resultant data files, locally written programs were used to segregate data for simple hydrogen bonds (D–H···X), for bifurcated hydrogen bonds (D–H···X(A)), and for hydrogen bonds that were trifurcated (D–H···X(A)(A')) or exhibited higher order multifurcation. Examples of typical searches are provided in the Supporting Information. The present paper focuses only on data for simple hydrogen bonds, D–H···X, in which each hydrogen atom interacts with a single halogen acceptor and with no other acceptors. Bifurcated and trifurcated hydrogen bonds will be discussed in a subsequent paper. It should be noted that the number of hydrogen atoms interacting with each halogen acceptor group (i.e., bifurcation at the acceptor) has not been examined in the present study.

Three geometric parameters have been used in the analysis of the hydrogen bonds, namely the H···X distance, the D–H···X angle, and the H···X–M or H···X–C angle. To compare the relative hydrogen bond acceptor capabilities of the halogens, the hydrogen bond distances for all donor–acceptor pairs have been put on a common scale by use of the normalized distance function $R_{\text{HX}} = d(\text{H}\cdots\text{X})/(r_{\text{H}} + r_{\text{X}})$, suggested by Lommerse et al.²⁴ This allows a qualitative assessment of the relative strengths of the different hydrogen bond types that are discussed. To investigate geometrical preferences, we have also adopted the approach of analyzing spatially normalized distance vs angle plots using the transformed coordinate system R_{HX}^3 vs $1 - \cos T$ ($T = 180 - (\text{D–H}\cdots\text{X})$), as described by Lommerse et al.,²⁴ since this removes the inherent statistical biases of conventional distance vs angle plots by ensuring that equal volumes of space are mapped onto equal areas of the two-dimensional plot. Some useful points of reference on these plots are as follows: $R_{\text{HX}}^3 = 1.0$ ($R_{\text{HX}} = 1.0$) corresponds to $d(\text{H}\cdots\text{X}) = \sum(r_{\text{H}} + r_{\text{X}})$; $1 - \cos T = 0.0$ corresponds to D–H···X = 180°, $1 - \cos T = 0.5$ corresponds to D–H···X = 120°, $1 - \cos T = 0.75$ corresponds to D–H···X = 104.5°, and $1 - \cos T = 1.0$ corresponds to D–H···X = 90° (Figures 1–3). The same correspondences arise between the angles H···X–M and H···X–C and the functions $1 - \cos A$ ($A = 180 - (\text{H}\cdots\text{X–M})$ and $A = 180 - (\text{H}\cdots\text{X–C})$, respectively) (Supplementary Figures S1 and S2). Histograms of the H···X–M and H···X–C angles (Figure 4) were plotted in 10° intervals and corrected for the sine-dependent geometric error in the frequency of observations that necessarily arises in sampling such angle data from crystal structures.²⁵

Theoretical Calculations

Electrostatic potentials were calculated at the Hartree–Fock level using the GAMESS-UK^{26a} package, employing the CEP (compact effective potential) pseudopotential of Stevens et al., and the associated VDZ basis set (SBKJC VDZ ECP)^{26b,f} for Pd and a Sadlej pVTZ (polarized valence triple- ζ) basis sets^{26c,f} on all other atoms. Geometries for the *trans*-PdX(CH₃)(PH₃)₂ model compounds were obtained by restricted-geometry optimization in which all bond lengths were optimized together with torsion angles involving methyl and phosphine hydrogen atoms. Interligand angles were maintained at 90°, and all non-hydrogen atoms were restricted to lie in the same plane. Geometries for the CH₃X compounds were obtained by full geometry optimization assuming C_{3v} molecular symmetry. All geometry optimizations were conducted at the Hartree–Fock level using GAMESS-UK with the following double- ζ basis sets for the metal complexes: SBKJC VDZ ECP^{26b,f} for Pd, Ahlrichs DZP^{26d,f} for C, H, F, Cl, and P, and Stuttgart RLC ECP DZP^{26e,f} for Br and I. Methyl halide geometries were obtained by optimization with the Sadlej pVTZ basis set for all atoms.

Results

The potential for hydrogen bond formation in the families of interactions D–H···X–M, D–H···X–C, and D–H···X[–] (D = C, N, O; X = F, Cl, Br, I; M = transition metal) has been assessed on the basis of intermolecular

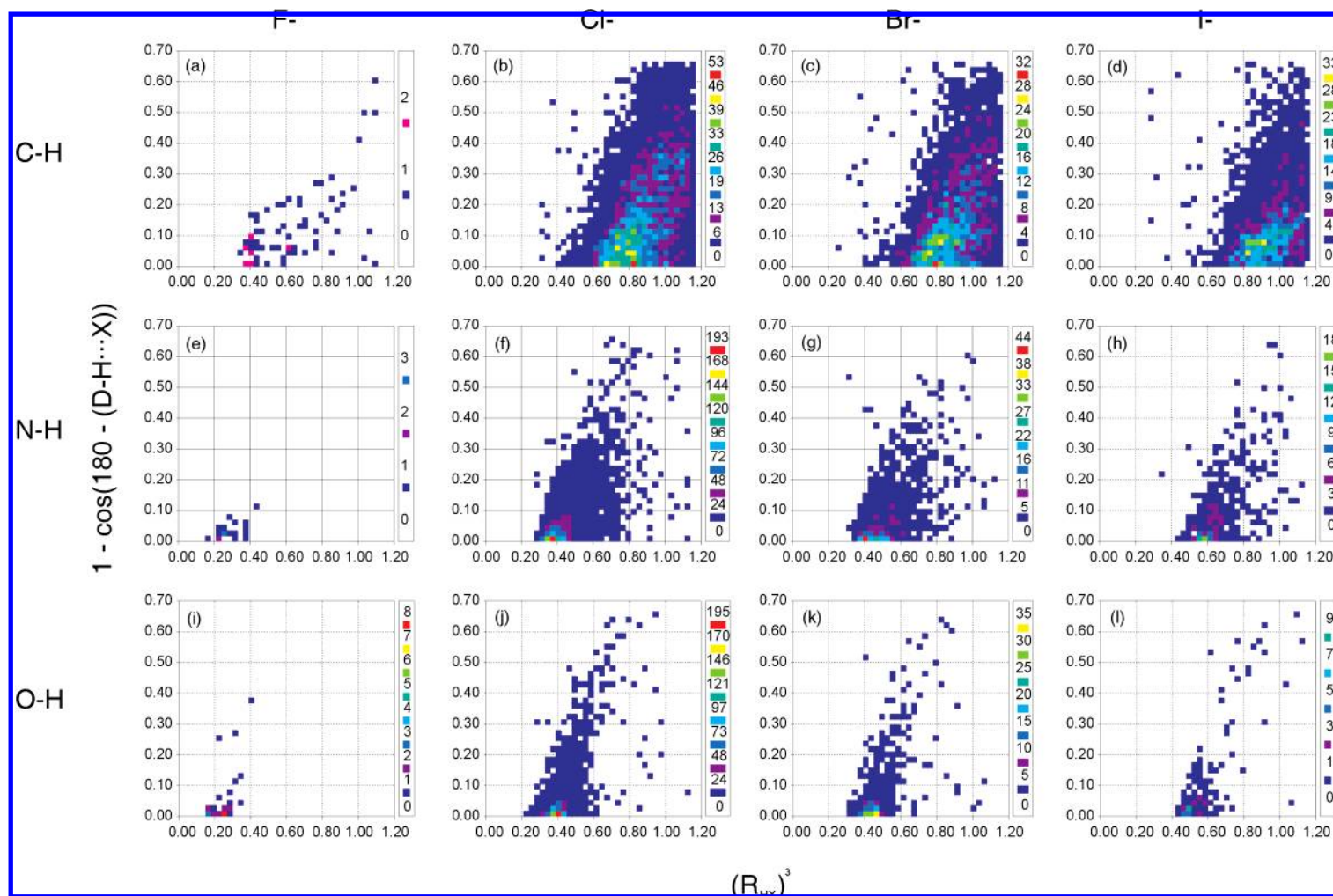


Figure 1. Spatially normalized plots of hydrogen bond distances (represented as R_{HX}^3) vs angle at the hydrogen (represented as $1 - \cos(180 - (D-H \cdots X))$) for $D-H \cdots X^-$ hydrogen bonds. Donors $D = C, N, O$ and acceptors $X = F, Cl, Br, I$ are as denoted for the rows and columns of this figure, respectively.

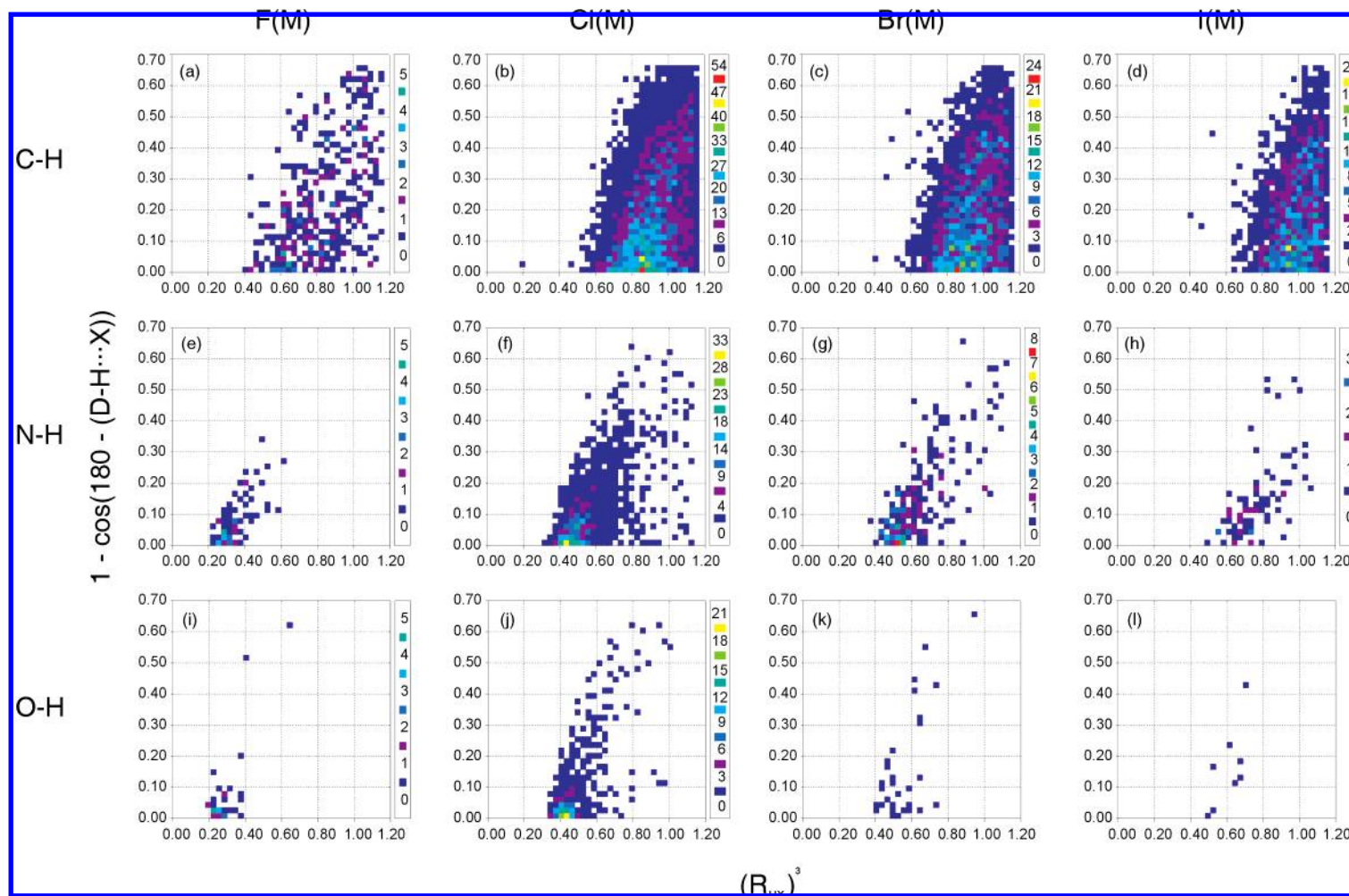


Figure 2. Spatially normalized plots of hydrogen bond distances (represented as R_{HX}^3) vs angle at the hydrogen (represented as $1 - \cos(180 - (D-H \cdots X))$) for $D-H \cdots X-M$ hydrogen bonds. Donors $D = C, N, O$ and acceptors $X = F, Cl, Br, I$ are as denoted for the rows and columns of this figure, respectively.

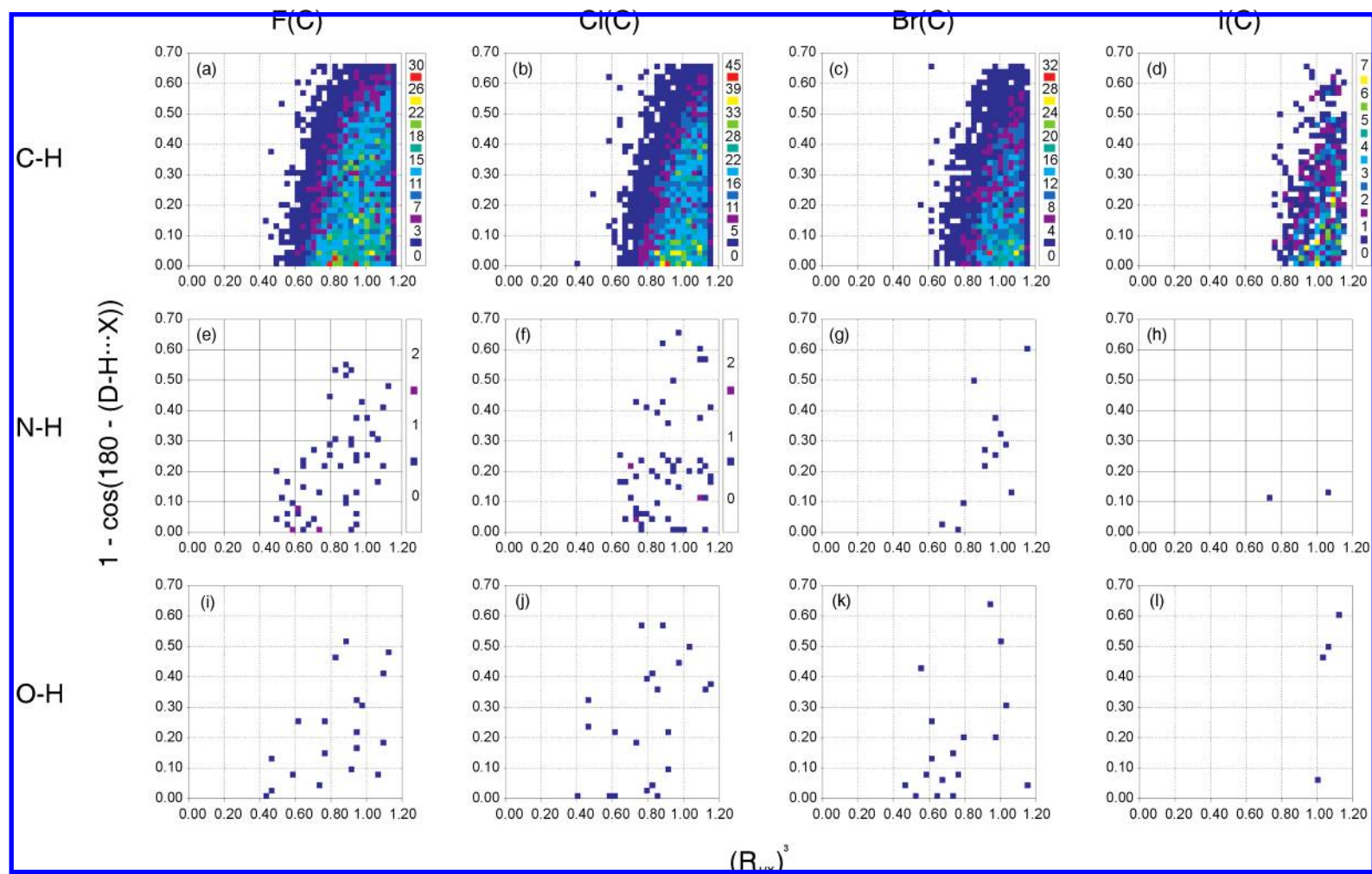


Figure 3. Spatially normalized plots of hydrogen bond distances (represented as R_{HX}^3) vs angle at the hydrogen (represented as $1 - \cos(180 - (D-H \cdots X))$) for $D-H \cdots X-C$ hydrogen bonds. Donors $D = C, N, O$ and acceptors $X = F, Cl, Br, I$ are as denoted for the rows and columns of this figure, respectively.

Table 1. Mean R_{HX} Distances for $\text{H}\cdots\text{X}$ Contacts with $R_{\text{HX}}^3 \leq 1.15$ ($R_{\text{HX}} < \text{ca. } 1.05$)

X	mean normalized distance, R_{HX} (no. of observns)		
	C–H \cdots X	N–H \cdots X	O–H \cdots X
F [−]	0.849 (69)	0.660 (19)	0.627 (32)
F–M	0.943 (374)	0.776 (73)	0.703 (37)
F–C	0.976 (7579)	0.923 (52)	0.930 (19)
Cl [−]	0.960 (8537)	0.768 (3834)	0.746 (2121)
Cl–M	0.975 (7943)	0.853 (1341)	0.799 (416)
Cl–C	0.995 (7729)	0.963 (55)	0.916 (21)
Br [−]	0.965 (4203)	0.811 (1082)	0.782 (529)
Br–M	0.982 (3269)	0.879 (205)	0.820 (30)
Br–C	0.998 (4018)	0.973 (12)	0.902 (17)
I [−]	0.982 (3538)	0.873 (434)	0.833 (141)
I–M	0.997 (2429)	0.923 (83)	0.868 (8)
I–C	1.006 (603)	<i>a</i>	<i>a</i>

^a Fewer than 5 observations.

geometric data from crystal structures. Further subdivision of the interactions by greater specification of the donor or acceptor environments has not been undertaken, except for exclusion of interactions that involve bifurcation at the hydrogen atom. A combination of $\text{H}\cdots\text{X}$ distance and $\text{D–H}\cdots\text{X}$ angle data has been used to assess whether each donor–acceptor combination exhibits behavior consistent with a hydrogen bond description. As noted earlier, the $\text{H}\cdots\text{X}$ distance data have been normalized ($R_{\text{HX}} = d(\text{H}\cdots\text{X})/(r_{\text{H}} + r_{\text{X}})$) to take account of the different sizes of the four halogens such that a direct comparison can be made between distance distributions for different halogens. The normalized distance data give a qualitative comparison of interaction strengths. The directionality of the halogen acceptors is examined for the case of the M–X and C–X systems using normalized histograms of $\text{H}\cdots\text{X–M}$ angles (and spatially corrected distance vs angle plots of R_{HX}^3 vs $1 - \cos(180 - (\text{H}\cdots\text{X–M}))$).

$\text{H}\cdots\text{X}$ (R_{HX}) Distances and $\text{D–H}\cdots\text{X}$ Angles. (a) $\text{D–H}\cdots\text{X}^-$ Interactions. The plots of R_{HX}^3 vs $1 - \cos(180 - (\text{D–H}\cdots\text{X}))$, shown in parts a–l of Figure 1, all have a similar appearance, such that at shorter $\text{H}\cdots\text{X}$ distances (smaller R_{HX}^3) the prevalent $\text{D–H}\cdots\text{X}$ angle is close to 180° (i.e., $1 - \cos(180 - (\text{D–H}\cdots\text{X}))$ close to zero). Furthermore, the region in which there is the greatest density of observations occurs at or very close to 180° . These are typical distributions for hydrogen bonds and clearly indicate the appropriateness of applying such a description to $\text{D–H}\cdots\text{X}^-$ interactions for O–H, N–H, and C–H donors. These distributions are particularly dramatic for the strongest hydrogen bonds of this type, namely N–H \cdots F[−] and O–H \cdots X[−], for which essentially all data lie in the range $0.0 \leq 1 - \cos(180 - (\text{D–H}\cdots\text{X})) \leq 0.1$ [$180 \geq \text{D–H}\cdots\text{X} \geq 154^\circ$]. Table 1 lists the mean normalized hydrogen bond distances, R_{HX} , for $\text{D–H}\cdots\text{X}^-$ hydrogen bonds (first line of data listed for each halogen, X). As might be anticipated, mean distances decrease with increasing polarity of the D–H bond, such that for a given halide ion O–H donors form slightly shorter interactions than N–H donors, which in turn form substantially shorter interactions than C–H donors: i.e., O–H \cdots X[−] < N–H \cdots X[−] << C–H \cdots X[−].

When the halide ion acceptors for a given donor are compared, normalized distances follow the trend $\text{H}\cdots\text{F}$

< $\text{H}\cdots\text{Cl}$ < $\text{H}\cdots\text{Br}$ < $\text{H}\cdots\text{I}$. However, the greatest difference is between fluoride and chloride acceptors and the next greatest between bromide and iodide, with the smallest difference being between chloride and bromide. Thus, a normalized distance trend of $\text{H}\cdots\text{F} \ll \text{H}\cdots\text{Cl} = \text{H}\cdots\text{Br} < \text{H}\cdots\text{I}$ is a more informative description. The consequences of this trend upon hydrogen bond strength will be discussed in the broader context of all the halogen acceptor environments (vide infra).

(b) $\text{D–H}\cdots\text{X–M}$ Interactions. The plots of R_{HX}^3 vs $1 - \cos(180 - (\text{D–H}\cdots\text{X}))$, presented in parts a–l of Figure 2, show behavior entirely analogous to that for the $\text{D–H}\cdots\text{X}^-$ interactions, indicative that C–H, N–H, and O–H donor groups are each capable of forming viable $\text{D–H}\cdots\text{X–M}$ hydrogen bonds in combination with all metal halide acceptors. Mean normalized hydrogen bond distances, R_{HX} , for $\text{D–H}\cdots\text{X–M}$ hydrogen bonds are provided in Table 1 (line 2). The trends in distances vs donor group and vs halogen have been previously described.^{1b} Here we note that the trends follow those of the $\text{D–H}\cdots\text{X}^-$ hydrogen bonds, both upon variation of the donor group, D–H, and upon variation of the halogen acceptor group, X–M. Direct comparison of X[−] and X–M acceptors for the same donor group and halogen suggests that the greatest differences arise for fluoride ion vs metal fluoride and the most similar behavior arises for iodide ion vs metal iodide.

(c) $\text{D–H}\cdots\text{X–C}$ Interactions. Plots of R_{HX}^3 vs $1 - \cos(180 - (\text{D–H}\cdots\text{X}))$ are presented in parts a–l of Figure 3. Two cases, N–H \cdots I–C and O–H \cdots I–C, are clearly ill-defined due to lack of data, two and four observations, respectively, and will not be discussed subsequently. The plots for N–H \cdots Br–C, O–H \cdots Cl–C, and O–H \cdots Br–C interactions suggest a slight preference for larger $\text{D–H}\cdots\text{X}$ angles. This is more clearly the case for N–H \cdots Cl–C, N–H \cdots F–C, and O–H \cdots F–C interactions. Clearer still is the trend for all C–H \cdots X–C interactions, where many more data are available. The plots for these cases clearly resemble those for X[−] and X–M acceptors. The overall inference from these data, consistent with analyses of other weak hydrogen bonds,^{18,27} is that $\text{D–H}\cdots\text{X–C}$ interactions are directional and by implication attractive in nature and thus best described as (weak) hydrogen bonds. This conclusion is not entirely in agreement with some prior work on $\text{D–H}\cdots\text{F–C}$ hydrogen bonds^{3a,b} and will be further discussed in light of other studies (vide infra). $\text{D–H}\cdots\text{X–C}$ hydrogen bonds are clearly longer than their counterparts involving X–M and X[−] acceptor groups, as seen from Table 1. Examination of the normalized hydrogen bond distances, R_{HX} , for $\text{D–H}\cdots\text{X–C}$ hydrogen bonds shows that the clearest trend arises for the C–H \cdots X–C interactions, where there are plentiful observations in each case. The trend follows that of the stronger $\text{D–H}\cdots\text{X–M}$ and $\text{D–H}\cdots\text{X}^-$ hydrogen bonds, such that there is a monotonic increase in mean distance on going from fluorine to iodine acceptors, but the greatest difference is between F–C and Cl–C and the next greatest difference is between Br–C and I–C. This trend is also found for N–H \cdots X–C (X = F, Cl, Br) interactions. However, the trend for O–H \cdots X–C (X = F, Cl, Br) interactions, O–H \cdots F–C > O–H \cdots Cl–C > O–H \cdots Br–C, appears anomalous, since it is the reverse of the previous cases with R_{HX} distances.

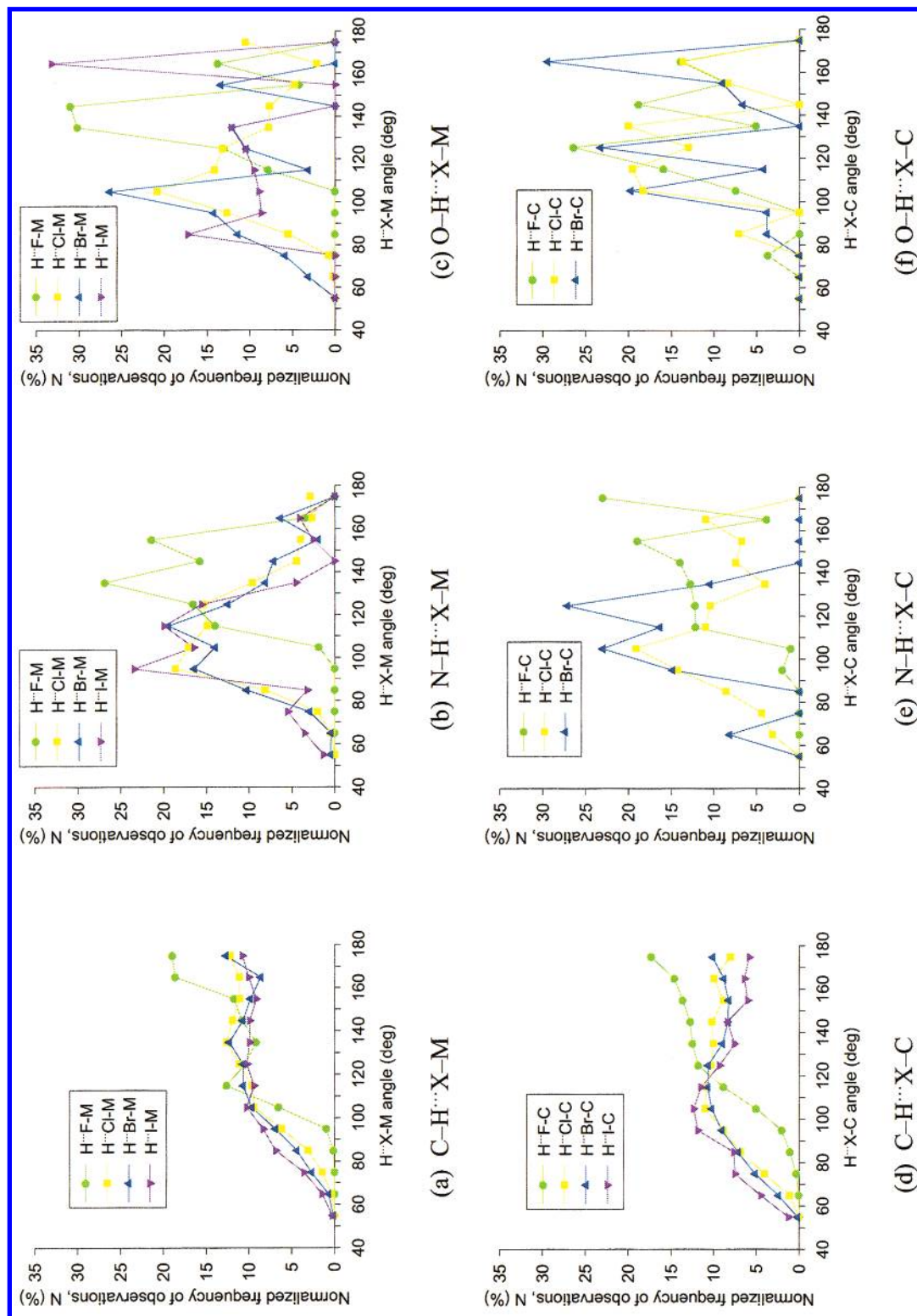


Figure 4. Normalized²⁵ distributions of H...X-M and H...X-C angles.

H··X–M and H··X–C Angles. (a) D–H··X–M Interactions. The distribution of H··X–M angles, corrected to account for the solid angle subtended at X, is provided as a set of histograms in parts a–c of Figure 4. As we have noted in a prior communication regarding N–H··X–M hydrogen bonds, metal fluorides show behavior different from that of the heavier halogens, in that typical H··F–M angles (120–160°) are larger than H··X–M angles (90–130° for X = Cl, Br, I).^{1b} This is illustrated in Figure 4b. Examination of Figure 4c shows that the same respective behavior is found for O–H··X–M hydrogen bonds.²⁸ Figure 4a shows that there is some similarity between C–H··X–M hydrogen bonds and their stronger counterparts, insofar as C–H··F–M interactions show a greater tendency toward larger H··F–M angles than do other C–H··X–M interactions (X = Cl, Br, I). However, the angular distributions are quantitatively dissimilar to those for D–H··X–M (D = N, O) hydrogen bonds, in that there is effectively no angular discrimination between 90 and 180° for C–H··X–M (X = Cl, Br, I), while most (C)H··F–M angles lie between 110 and 180°, with an apparent preference for angles of 160–180°.

(b) D–H··X–C Interactions. The corresponding (spatially corrected) distributions of H··X–C angles are shown in parts d–f of Figure 4. Figure 4d, which is based upon a large number of observations, indicates a slight preference for (C)H··X–C angles in the range 90–130° over larger angles, where X = Cl, Br, and a more pronounced preference for X = I, while (C)H··F–C angles mostly lie in the range 110–180° with an increasing preference at larger angles. These distributions resemble those for C–H··X–M interactions (Figure 4a), at least in the distinction between the behavior of fluorine and that of the other halogens. More striking, however, is the similarity between the C–H··X–C distributions and those observed for N–H··X–M and O–H··X–M interactions (Figure 4b,c). There is an even greater correspondence between the (N)H··X–C distributions, X = F, Cl, Br (Figure 4e), and the corresponding (N)H··X–M distributions (Figure 4b). The (O)H··F–C and (O)H··Cl–C angle distributions in Figure 2f also resemble the corresponding distributions in Figure 4b,c,e, though the (O)H··Br–C distribution does not appear to show any clear angular preferences. It should be noted with regard to the O–H··X–C interactions that only ca. 20 observations constitute the data set for each halogen.

Discussion

D–H··X Interactions: Are They Hydrogen Bonds?

Consideration of the correlated trends in hydrogen bond distance, H··X or R_{HX} , and D–H··X angle, expressed in the unbiased spatially normalized plots of R_{HX}^3 vs $1 - \cos(180 - (D-H\cdots X))$, leaves no doubt that all donor groups considered, C–H, N–H, and O–H, are able to form hydrogen bonds with all acceptor groups considered, X[−], X–M, and X–C (X = F, Cl, Br, I). This is evident from the tendency for larger D–H··X angles (i.e., closer to 180°) to be observed for shorter H··X (R_{HX}) separations^{18,27} (Figures 1–3).

Thus, halogens are able to engage in hydrogen bonds that involve the combination of strong donors with

strong acceptors (D–H··X[−] and D–H··X–M, D = N, O), weak donors with strong acceptors (C–H··X[−] and C–H··X–M), strong donors with weak acceptors (D–H··X–C, D = N, O), and weak donors with weak acceptors (C–H··X–C), which span an estimated energy scale of ca. 0.2 kcal/mol for the weaker C–H··X–C hydrogen bonds (e.g. 0.2 kcal/mol calculated for CH₄··FCH₃)^{3b} to ca. 25 kcal/mol for O–H··F[−] (e.g. 23.3 kcal/mol experimental and 27.3 kcal/mol calculated for OH₂··F[−]).²⁹

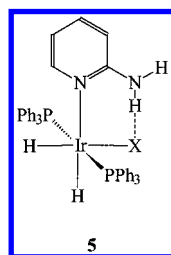
Hydrogen Bond Distances and Strengths. On the basis of the geometries reported above, the behavior of fluorine-containing hydrogen bond acceptors clearly differs from that of the other halogens. Not only are mean *normalized* distances, R_{HX} , shortest for X = F, but the angular distribution of hydrogen bond donors, D–H, about F–M and F–C bonds differs from that about other X–M and X–C bonds (vide supra).

The trend in increasing mean R_{HX} distance such that H··F ≪ H··Cl ≤ H··Br < H··I is evident for both halide (X[−]) and metal halide (X–M) acceptors for all donor groups, D–H (D = C, N, O). Remarkably, the same trend is found for C–H··X–C interactions and appears to be present for N–H··X–C interactions (X = F, Cl, Br), though a reversed (apparently anomalous) trend is observed for O–H··X–C interactions. There is also a clear trend for all halogen environments of decreasing mean R_{HX} upon increasing the polarity of the donor group, such that (C)H··X ≫ (N)H··X > (O)H··X. The only exceptions again arise for the O–H··X–C interactions. Indeed, the data as a whole suggest that the mean R_{HX} value for O–H··F–C is overestimated and that those for O–H··Cl–C and O–H··Br–C interactions are underestimated.³⁰ The third trend in mean R_{HX} that can clearly be discerned is that D–H··X[−] < D–H··X–M ≪ D–H··X–C for all halogens, consistent with our earlier report on the hydrogen bonding ability of chlorine.^{1a}

In two previous surveys of geometries of hydrogen bonds involving halide ions the authors have taken an approach slightly different from to ours, focusing more upon the variation of donor groups rather than simply the donor atom as in the present study.² The survey by Steiner^{2b} provides an up-to-date tabulation of mean H··X and D··X distances for a wide variety of donor groups, including a detailed subdivision of the distributions for donor atoms C, N, and O. The survey by Mascial^{2a} focuses on O–H, N–H⁺, and N–H donors. In neither case is an H··X distance normalization applied. Thus, the present study is complementary to these prior reports in that it focuses on direct comparison of the hydrogen bond acceptor capability of the halide ions through the use of normalized hydrogen bond distances, R_{HX} . The halide ion data also provide a benchmark for comparison with the data for metal halide (X–M) and halocarbon (X–C) acceptors.

Returning to the earlier observation that mean R_{HX} distances follow the trend H··F ≪ H··Cl ≤ H··Br < H··I for a given donor group and acceptor type (X[−], X–M, or X–C), the implications are that the trend in hydrogen bond strength should be H··F ≫ H··Cl = H··Br > H··I. That this is the case is reinforced by consideration of a study by Crabtree, Eisenstein, and co-workers in which the N–H··X–Ir hydrogen bond

strengths in **5** have been determined in solution by an



elegant combination of NMR methods and *ab initio* calculations.³¹ The trend in the values obtained, 5.2 kcal/mol (X = F), 2.1 kcal/mol (Cl), 1.8 kcal/mol (Br), and < 1.3 kcal/mol (I), is in excellent qualitative agreement with that derived from our consideration of normalized hydrogen bond distances.

Anisotropic Acceptor Behavior of Terminally Bound Halogens. It has previously been noted^{1b} (vide supra) that terminal metal halides exhibit preferential angles of approach of strong hydrogen bond donors (N–H) and that the behavior of metal fluorides ($H\cdots F-M = 120-160^\circ$) is distinct from that of the heavier halogens ($H\cdots X-M = 90-130^\circ$).^{1b} The broader questions prompted by this observation are (1) why does this anisotropy occur, (2) is it present for weaker donors, i.e., $C-H\cdots X-M$, and (3) does it also occur for organic halides (X–C)?

Focusing first upon the metal halide systems, it seems reasonable to assume that the electrostatic component of the $D-H\cdots X-M$ hydrogen bond energy is dominant. Thus, we have explored the electronic origins of the $H\cdots X-M$ angle anisotropy by considering the electrostatic potential in the vicinity of the terminal halide ligand, X, in a series of model systems, *trans*-PdX(CH₃)(PH₃)₂, as calculated by Hartree–Fock methods³² (see Experimental Section). Figure 5 shows the negative region of the potential associated with this series of compounds. In each case the region of negative potential lies in the vicinity of the halogen. The angle subtended at the halogen by the points of minima in the electrostatic potential should then represent the preferred approach of hydrogen bond donors, assuming that the electrostatic component of the $D-H\cdots X-M$ hydrogen bond energy is dominant. These angles (see Table 2) are in good agreement with the preferred $H\cdots X-M$ angles presented in Figure 4 and clearly indicate that the anisotropic hydrogen bond acceptor behavior associated with the terminal metal halides is predominantly electronic rather than steric³³ in origin. The depths of the potential minima also demonstrate why the fluoride ligand forms much stronger hydrogen bonds than the other halide ligands. This is of course associated with the greater electronegativity of fluorine and thus M–X bond polarity, leading to a greater accumulation of negative charge on the fluoride ligand than for its heavier halogen counterparts. It is also noteworthy that while the potential minima are well resolved for PdCl(CH₃)(PH₃)₂, PdBr(CH₃)(PH₃)₂, and PdI(CH₃)(PH₃)₂, the minima are almost unresolved for PdF(CH₃)(PH₃)₂. This suggests that the $H\cdots X-M$ angular preference should be more pronounced for the three heavier halogens but less well-defined for the metal fluoride case.

Examination of the molecular orbitals for the model systems reveals the source of angular discrimination (or

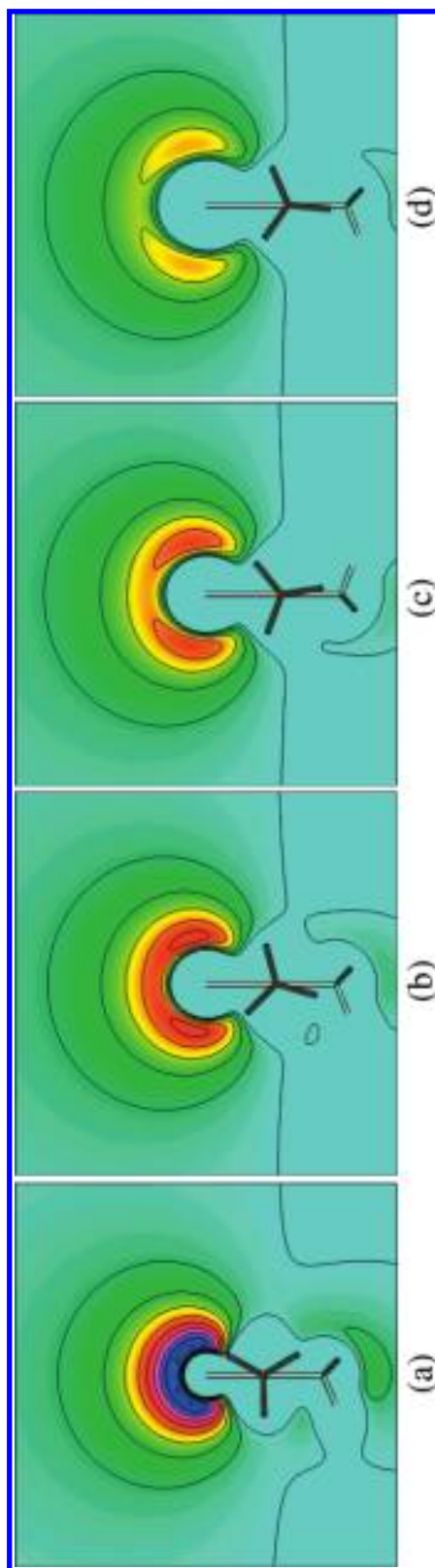


Figure 5. Negative electrostatic potential contoured at 10 kcal/mol intervals for *trans*-PdX(Me)(PH₃)₂: (a) X = F; (b) X = Cl; (c) X = Br; (d) X = I.

Table 2. Data for Calculated Electrostatic Potential in the Vicinity of the Halogen for *trans*-PdX(Me)(PH₃)₂ and CH₃X Model Systems

	in PdXCP ₂ molecular plane (cf. Figure S3)		in orthogonal plane through C–Pd–X (cf. Figure 5)		H–C–X plane in CH ₃ X (cf. Figure 6)	
	potential minimum (kcal/mol)	Pd–X···min ^a angle (deg) and angle range ^b for min + 1 kcal/mol	potential minimum (kcal/mol)	Pd–X···min angle (deg) and angle range ^b for min + 1 kcal/mol	potential minimum (kcal/mol)	C–X···min angle (deg) and angle range ^b for min + 1 kcal/mol
X = F	–89.8	155 (130–180) ^b	–91.5	131 (120–151) ^b	–30.9	127 (115–141) ^b
X = Cl	–49.0	124 (113–140) ^b	–53.2	110 (97–121) ^b	–19.3	107 (97–117) ^b
X = Br	–42.5	124 (110–136) ^b	–46.9	106 (93–120) ^b	–17.2	104 (95–114) ^b
X = I	–33.9	121 (109–136) ^b	–37.5	106 (93–120) ^b	–14.1	105 (95–114) ^b

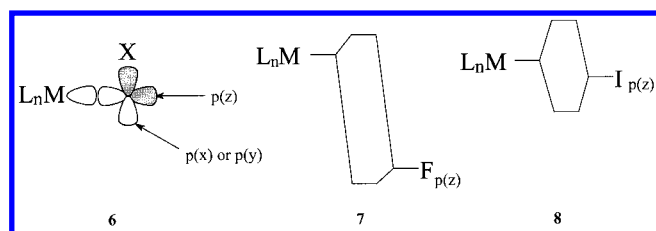
^a These angles are larger than those in the orthogonal plane due to the effect of the positive electrostatic potential from the PH₃ ligands that lie in the molecular plane. ^b Potential minimum varies by only ca. 1 kcal/mol over this angular range, indicating that the potential well is more flat-bottomed for X = F than for X = Cl, Br, I.

Table 3. Population Difference between Axial (p_z) and Non-axial (p_x, p_y) Halogen p Orbital Basis Functions for *trans*-PdX(Me)(PH₃)₂ and CH₃X Model Systems^a

	population (e) (p _x + p _y)/2 – p _z		population (e) (p _x + p _y)/2 – p _z
PdF(Me)(PH ₃) ₂	0.094	CH ₃ F	0.351
PdCl(Me)(PH ₃) ₂	0.223	CH ₃ Cl	0.583
PdBr(Me)(PH ₃) ₂	0.267	CH ₃ Br	0.622
PdI(Me)(PH ₃) ₂	0.300	CH ₃ I	0.679

^a Populations are summed over all basis functions of the same symmetry using the Sadlej basis sets.

lack thereof) at the halogens. This can be explained by envisioning a simplified model for M–X bonding in which a σ -bond is formed between the axial p orbital, p_z, of a halide ion and an appropriate d orbital from the metal fragment (**6**). For the M–F bond (**7**) the bonding



orbital will be primarily fluorine p in character, due to the substantial difference in electronegativity between a transition metal and fluorine. Expressed another way, there would be little donation of electron density from the (filled) fluoride p orbital to the metal. The other extreme is the M–I bond (**8**), which is more covalent in character, the bonding orbital possessing substantially shared metal and iodine orbital character. Thus, in comparison to the M–F case, there is now appreciable donation of electron density from the halide (iodide) ion p orbital to the metal.

This is confirmed by orbital population analysis (Table 3). Such electron donation depletes the charge density in the vicinity of the halogen trans to the metal, relative to that of a spherical halide ion. This charge density depletion is clearly manifested in the electrostatic potentials shown in Figure 5. Thus, this simple orbital model rationalizes not only the anisotropy of the heavier halogen acceptors (Cl, Br, and I) but also the fact that metal fluorides exhibit larger H···X–M angles and indeed less directional preference in the angle of approach of hydrogen bond donors. Terminal metal fluo-

rides might thus be considered to behave as only slightly perturbed halide ions, whereas this is not the case for the heavier halogens.

The next question posed was whether the same acceptor anisotropy observed for strong donors is present (or observable) for weak donors. Here it is instructive to consider the now extensive literature on D–H···O hydrogen bonds (D = C, N, O). A number of studies in recent years have shown that hydrogen bonds involving weaker C–H donors exhibit geometric characteristics qualitatively similar to those of the analogous systems involving stronger N–H and O–H donors. The main differences that arise are that C–H donors form hydrogen bonds with much longer hydrogen bond distances and the angular characteristics are less sharply defined, since of course weaker hydrogen bonds are more subject to deformation due to competition with other forces in the solid state (the source of most geometric data).¹⁸ However, in their recent monograph on weak hydrogen bonds, Desiraju and Steiner note,¹⁸ for perhaps the most well-studied weak hydrogen bond, C–H···O=C, that although no systematic study of H···O=C angle distribution (i.e., acceptor anisotropy) has been undertaken,³⁴ the consensus is that the distribution lies around a preferred angle of 120°, consistent with analyses of the analogous strong hydrogen bonds, D–H···O=C (D = N, O).

Comparing C–H···X–M with N–H···X–M and O–H···X–M hydrogen bonds, the same conclusions as reached for D–H···O hydrogen bonds¹⁸ appear to apply when considering hydrogen bond distances H···X (or R_{HX}) or D–H···X angles, as noted above. However, consideration of H···X–M angles shows that the angular preference for C–H donors (Figure 4a) resembles that for stronger N–H (Figure 4b) and O–H (Figure 4c) donors only inasmuch as H···F–M angles tend to be larger than other H···X–M angles. The distinct angular preference (90–130° for X = Cl, Br, I) exhibited for stronger donors is not evident for C–H donors. Nevertheless, these observations combined with “chemical common sense” suggest that C–H···X–M hydrogen bonds behave in an analogous manner to the stronger N–H···X–M and O–H···X–M hydrogen bonds.

Let us now consider the case for weak acceptors, i.e., the H···X–C angle distribution for D–H···X–C hydrogen bonds. Turning first to the strong donors, D = N, O, the angle distribution for N–H···X–C hydrogen

bonds (Figure 4e)³⁵ is very similar to that for the N–H···X–M (Figure 4b) and O–H···X–M (Figure 4c) cases. Furthermore, O–H···Cl–C hydrogen bonds (Figure 4f) exhibit a preference for H···Cl–C angles in the range 100–140°, consistent with prior observations for the behavior of metal chloride acceptors. However, for O–H···Br–C and O–H···F–C interactions the trends in H···X–C angle do not so closely follow those of the corresponding H···X–M angles.³⁵ As we turn to the combination of weak donors and weak acceptors, i.e., C–H···X–C hydrogen bonds (Figure 4d), it is remarkable to see that there is a distinct preference for H···X–C angles in the 90–130° range, where X = Cl, Br, I. For X = F, there is a marked preference for larger H···F–C angles (>120°) and a close resemblance to the distribution for C–H···F–M hydrogen bonds (Figure 4a).

The similarity of the H···X–C angle distributions to the corresponding H···X–M angle distributions in most cases strongly suggests that the acceptor behavior of the halogens is analogous in the two environments. This argument is reinforced by examination of the electrostatic potential surrounding the halogen in the methyl halides (Figure 6). For the heavier halogens, i.e., CH₃X (X = Cl, Br, I), well-resolved potential minima are observed, analogous to the case for PdX(Me)(PH₃)₂ (X = Cl, Br, I). The location and width of the potential wells suggest that the formation of D–H···X–C hydrogen bonds with geometries of ca. 90 < H···X–C < 130° should be favored, consistent with the observed H···X–C angle distributions. The potential minima for CH₃F are less well resolved but are superimposed on an overall potential that is more negative than that of its heavier halogen congeners. This suggests a stronger overall interaction but with less distinct H···F–C angles. The locations of the minima also suggest that the H···F–C angles should typically be larger than H···X–C angles (X = Cl, Br, I) (Table 2).

There is remarkably good qualitative correspondence between the potential distributions of the methyl halides and the corresponding metal halides,³⁶ the potential being more negative for the metal halides due to the more polar M–X bond arising from the greater difference in electronegativities between X and M than between X and C. However, while the potential minima for CH₃F are less well resolved than for CH₃X (X = Cl, Br, I), they are better resolved than for Pd(PH₃)₂(CH₃)F. This most probably results from the greater covalency of the F–C bonds compared with F–M, which also manifests itself in greater donation of electron density from the axial fluorine p_z orbital to carbon and thus a greater distinction between axial and nonaxial fluorine p-orbital populations (Table 3).

Relationship between H···X and M···X Interactions. Hydrogen bonds are an example of a Lewis acid–Lewis base interaction, the Lewis acid being the proton donor and the Lewis base being the proton acceptor. Thus, one might envision that detailed analysis of hydrogen bonding interactions should also be pertinent to the study of interactions of the same Lewis bases with certain other Lewis acids. Indeed, the generality of the orbital description of three-center interactions has been described recently by Hoffman,³⁷ and the relationship

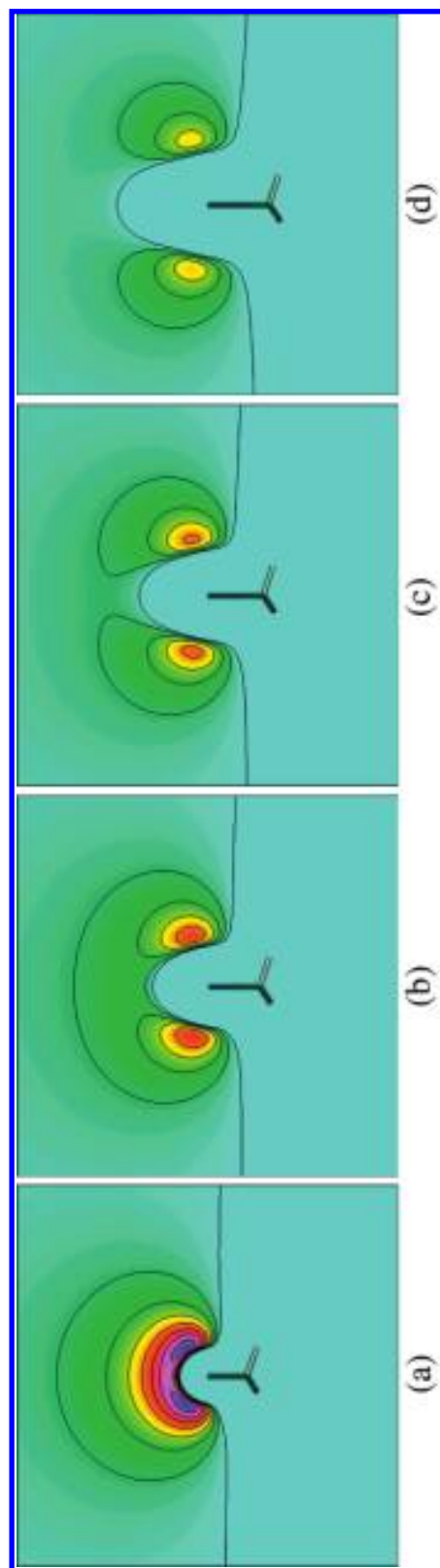


Figure 6. Negative electrostatic potential contoured at 4 kcal/mol intervals for CH₃X: (a) X = F; (b) X = Cl; (c) X = Br; (d) X = I.

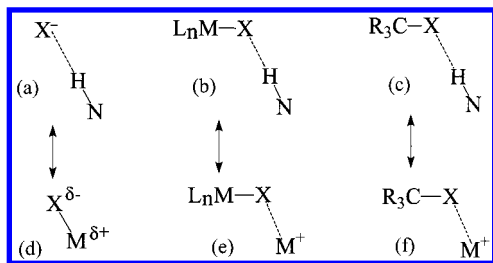


Figure 7. Correspondence between $H\cdots X$ and $M\cdots X$ interactions: (a) halide ion hydrogen bond acceptor; (b) metal halide hydrogen bond acceptor; (c) halocarbon hydrogen bond acceptor; (d) terminal metal halide; (e) bridging metal halide; (f) halocarbon coordination complex.

between the interactions of hydrogen bond donors or metal ions with carbonyl ligands has also been explored.^{34c,38}

With regard to the present halogen-containing Lewis bases, it is instructive to examine the correspondence between the interactions of hydrogen bond donors, $D-H$, and that of metal centers, M^{n+} or ML_n , as illustrated in Figure 7. The relationship between $D-H\cdots X^-$ hydrogen bonds (Figure 7a) and $M-X$ bonds (Figure 7d) is straightforward. $M-X$ bonds are of course generally stronger by some tens of kcal/mol, and while $D-H\cdots X^-$ hydrogen bonds can be understood almost purely in electrostatic terms, the orbital descriptions of the two interactions are very similar, viz. a filled halide orbital interaction with a vacant $D-H$ σ^* orbital or with a vacant metal orbital.

In a comparison of $D-H\cdots X-M$ hydrogen bonds (Figure 7b) and $M-X-M$ bonds (Figure 7e), again analogous orbital descriptions can be used to characterize the two systems. The similarity of the two interactions is further reinforced by consideration of binary metal halides,³⁹ for which bridging chlorides, bromides, and iodides almost universally adopt $M-X-M$ angles far removed from linearity, whereas there are a number of examples of systems containing linear $M-F-M$ arrangements (Figure 8).

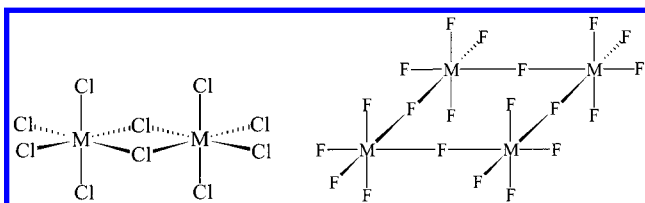


Figure 8. Molecular units of the structures of MX_5 ($M = Nb, Ta$) highlighting the different bridging modes adopted by Cl (angular) and F (linear).

Turning finally to halocarbon Lewis bases, reviews by Kulawiec and Crabtree⁴⁰ and more recently by Plenio⁴¹ indicate the scope of $M\cdots X-C$ interactions (Figure 7f) involving both main-group metals, especially groups 1 and 2, and transition metals. Data on the strength of $M\cdots X-C$ interactions are sparse, but one would anticipate that these are stronger than $D-H\cdots X-C$ hydrogen bonds (<3 kcal/mol). Indeed they can in some instances be much stronger, viz. 31 kcal/mol for $[CH_3F-Li]^+$.⁴² In the aforementioned reviews, Kulawiec and Crabtree note that the $M\cdots X-C$ angle is typically close to 90° . Plenio notes that, for metals for which

crystallographically characterized $M\cdots F-C$ interactions are the most abundant, angles typically lie in the following ranges: $Na\cdots F-C = 100-120^\circ$, $K\cdots F-C = 100-130^\circ$, $Cs\cdots F-C = 90-140^\circ$, $Ag\cdots F-C = 100-120^\circ$. Strauss has also observed $Li\cdots F-C$ angles to predominantly lie in the range $100-120^\circ$ in a series of related salts of fluorinated phenoxides.⁴² However, these reports provide an incomplete assessment of $M\cdots X-C$ geometries. Using the CSD to survey these angle trends for each halogen and for main group or transition metals suggests⁴³ that $M\cdots X-C$ angles from 90 to 120° predominate for $X = Cl, Br, I$. However, although similar geometries are most common for fluorocarbon complexes, larger $M\cdots F-C$ angles occur far more frequently than larger $M\cdots X-C$ angles ($X = Cl, Br, I$). Clearly a more detailed study of the geometries of $M\cdots X-C$ interactions is needed, but it appears at this time as if there are many similarities between $D-H\cdots X-C$ hydrogen bonds and $M\cdots X-C$ interactions. One apparent difference, however, is that $M\cdots X-C$ bond strength is well-established to follow the trend with X : $X = I > Br > Cl > F$. In contrast, the distance data reported herein for $D-H\cdots X-C$ interactions suggests that the trend in hydrogen bond strength follows the order $F > Cl > Br > I$.

Main Group Metal Halides. Halogens form compounds with virtually all main group elements, though the hydrogen bonding ability of such a broad range of halogen environments has not been considered in the present study. Nevertheless, preliminary investigation using the CSD of the geometries of interaction between the strong hydrogen bond donors $N-H$ and $O-H$ with group 14 halides, $Si-X$, $Ge-X$, and $Pb-X$, suggests⁴³ that the behavior is rather similar to that with transition metal halides, $M-X$.

Of special noteworthiness among main group halide compounds are the anions BF_4^- and PF_6^- , due to their abundance as counterions to organometallic cations. The fluoride substituents of the anions appear to be capable of forming moderately strong hydrogen bonds, aided by negative charge associated with the anions. Most abundant are charge-assisted $C-H\cdots F-B$ ⁴⁴ or $C-H\cdots F-P$ ⁴⁵ hydrogen bonds. The anions BF_4^- and PF_6^- are among the earlier examples of so-called weakly coordinating anions, i.e. anions that interact only weakly with electrophilic metal centers. Among the newer generations of "super-weak" anions are the partially halogenated or perhalogenated carboranes, prototypical of which would be $CB_{11}H_{11-n}X_n^-$.⁴⁶ One would anticipate the halogen substituents of these anions to serve as only very weak hydrogen bond acceptors, but clearly the results of the present study are pertinent to the understanding of the interactions with Lewis acids of these anions and of other weakly coordinating ions, most of which have a highly fluorinated periphery.⁴⁷

Summary, Broader Relevance, and Future Studies

The present study clearly establishes halogen atoms as potential hydrogen bond acceptors when present as halide ions, metal halides, or halocarbons, and able to interact with both strong and weak hydrogen bond donors. Preferred geometries have been determined for all of these interactions, and the underlying reasons for

these preferences have been established. The study should be of general relevance in the understanding of weak interactions that are now recognized to be important to so many areas of chemistry and structural biology.¹⁸ The results are of specific relevance to the fields of crystal engineering and supramolecular chemistry. As noted previously, efforts to exploit the strong, directional hydrogen bond capability of metal-bound halogens in crystal engineering have led to some recent successes.^{16,17} Recent reports have also begun to show the importance of much weaker hydrogen bonds involving halocarbon acceptors in controlling packing arrangements in the solid state (i.e., C–H···X–C; X = F,^{3f} Cl,⁴⁸ Br⁴⁸) and in influencing the nucleation stage of crystal growth in solutions using halogenated solvents (e.g., O–H···Cl–C interactions in the nucleation of 2,6-dihydroxybenzene crystals in CHCl₃ solution⁴⁹).

We are presently exploring the preferences exhibited by bifurcated and trifurcated hydrogen bonds involving halogens using methods similar to those presented herein. In addition, we have begun to apply this knowledge of preferred geometries to improve our design efforts in the areas of crystal engineering and supramolecular assemblies based upon hydrogen bonding involving halometalate anions.¹⁶

Note Added in Revision. After this paper was accepted, a paper by Thallapally and Nangia⁵⁰ was published describing an analysis very similar to those we have conducted, but restricted to C–H···Cl[–], C–H···Cl–M, and C–H···Cl–C interactions. Their conclusions differ somewhat from ours. They suggest that in contrast to the weak hydrogen bonds formed by the halide and metal halide (Cl–M) acceptors, C–H···Cl–C interactions are essentially van der Waals contacts. Our results, using normalized geometry plots with all bifurcated interactions removed, indicate that C–H···Cl–C interactions have the characteristics of very weak hydrogen bonds (in particular, see Figure 3b and compare with Figures 1b and 2b). What is in no doubt is that we are clearly reaching the limit of hydrogen bond behavior when considering interactions of the type C–H···X–C (X = halogen).

Acknowledgment. L.B. and E.A.B. are grateful to Karl Kedrovsky for programming assistance and to the University of Missouri–St. Louis and National Science Foundation (Grant No. CHE-9988184) for financial support. L.B. and P.S. thank NATO (Grant No. CRG-920164) for support of their collaboration.

Supporting Information Available: Plots of R_{HX}^3 vs $1 - \cos(180 - (H \cdots X - M))$ and R_{HX}^3 vs $1 - \cos(180 - (H \cdots X - C))$ for all donor and acceptor groups, alternative views of the electrostatic potentials for compounds PdX(CH₃)(PH₃)₂ and CH₃X, examples of input files for CSD searches, and molecular geometries resulting from optimizations. This material is available free of charge via the Internet at <http://pubs.acs.org>.

References

- (1) (a) Aullón, G.; Bellamy, D.; Brammer, L.; Bruton, E. A.; Orpen, A. G. *Chem. Commun.* **1998**, 653. (b) Brammer, L.; Bruton, E. A.; Sherwood, P. *New J. Chem.* **1999**, 23, 965.
- (2) (a) Mascall, M. J. *Chem. Soc., Perkin Trans. 2* **1997**, 1999. (b) Steiner, T. *Acta Crystallogr.* **1998**, B54, 456.
- (3) (a) Dunitz, J. D.; Taylor, R. *Chem. Eur. J.* **1997**, 3, 89. (b) Howard, J. A. K.; Hoy, V. J.; O'Hagan, D.; Smith, G. T. *Tetrahedron* **1996**, 52, 12613. (c) Murray-Rust, P.; Stallings, W. C.; Monti, C. T.; Preston, R. K.; Glusker, J. P. *J. Am. Chem. Soc.* **1983**, 105, 3206. (d) Shimoni, L.; Carrell, H. L.; Glusker, J. P.; Coombs, M. M. *J. Am. Chem. Soc.* **1994**, 116, 8162. (e) Shimoni, L.; Glusker, J. P. *Struct. Chem.* **1994**, 5, 383. (f) Thalladi, V. R.; Weiss, H.-C.; Bläser, D.; Boese, R.; Nangia, A.; Desiraju, G. R. *J. Am. Chem. Soc.* **1998**, 120, 8702.
- (4) Hille, B. *Ionic Channels of Excitable Membranes*; Sinauer Associates: Sunderland, MA, 1992.
- (5) (a) Shionoya, M.; Furuta, H.; Lynch, V.; Harriman, A.; Sessler, J. L. *J. Am. Chem. Soc.* **1992**, 114, 5714. (b) Edema, J. J. H.; Libbers, R.; Ridder, A. M.; Kellogg, R. M.; van Bolhuis, F.; Kooijman, H.; Spek, A. L. *J. Chem. Soc., Chem. Commun.* **1993**, 625. (c) Pascal, R. A., Jr.; Ho, D. M. *Tetrahedron* **1994**, 50, 8559. (d) Kavallieratos, K.; de Gala, S. R.; Austin, D. J.; Crabtree, R. H. *J. Am. Chem. Soc.* **1997**, 119, 2325. (e) Kavallieratos, K.; Bertau, C. M.; Crabtree, R. H. *J. Org. Chem.* **1999**, 64, 1675. (f) Shukla, R.; Kida, T.; Smith, B. D. *Org. Lett.* **2000**, 2, 3099. (g) Choi, K.; Hamilton, A. D. *J. Am. Chem. Soc.* **2001**, 123, 2456.
- (6) (a) Deetz, M. J.; Shang, M. Smith, B. D. *J. Am. Chem. Soc.* **2000**, 122, 6201. (b) Redman, J. E.; Beer, P. D.; Dent, S. W.; Drew, M. G. B. *Chem. Commun.* **1998**, 231. (c) Cooper, J. B.; Drew, M. G. B.; Beer, P. D. *J. Chem. Soc., Dalton Trans.* **2001**, 392.
- (7) (a) Vilar, R.; Mingos, D. M. P.; White, A. J. P.; Williams, D. *J. Angew. Chem., Int. Ed.* **1998**, 37, 1258. (b) Fleming, J. S.; Mann, K. L. V.; Carraz, C.-A.; Psillakis, E.; Jeffrey, J. C.; McCleverty, J. A.; Ward, M. D. *Angew. Chem., Int. Ed.* **1998**, 37, 1279. (c) Mareque Rivas, J. C.; Brammer, L. *New J. Chem.* **1998**, 22, 1315.
- (8) Bentrup, U.; Feist, M.; Kemnitz, E. *Prog. Solid State Chem.* **1999**, 27, 75.
- (9) (a) Babar, M. A.; Larkworthy, L.; Tandon, S. S. *J. Chem. Soc., Dalton Trans.* **1983**, 1081. (b) Bonamartini-Corradi, A.; Battaglia, L. P.; Rubenacker, J.; Willett, R. D.; Grigereit, T. E.; Zhou, P.; Drumheller, J. E. *Inorg. Chem.* **1992**, 31, 3859.
- (10) Riley, M. J.; Neill, D.; Bernhard, P. V.; Byriel, K. A.; Kennard, C. H. L. *Inorg. Chem.* **1998**, 37, 3635.
- (11) (a) For a discussion of the protonation of metal halides, see: Kuhlman, R. *Coord. Chem. Rev.* **1997**, 167, 205. (b) Yandulov, D. V.; Caulton, K. G.; Belkova, N. V.; Shubina, E. S.; Epstein, L. M.; Khoroshum, D. V.; Musae, D. G.; Morokuma, K. *J. Am. Chem. Soc.* **1998**, 120, 12553.
- (12) (a) Murphy, V. J.; Hascall, T.; Chen, J. Y.; Parkin, G. *J. Am. Chem. Soc.* **1996**, 118, 7428. (b) Jassim, N. A.; Perutz, R. N. *J. Am. Chem. Soc.* **2000**, 122, 8685.
- (13) (a) Lee, D.-H.; Kwon, H. J.; Patel, B. P.; Liable-Sands, L. M.; Rheingold, A. L.; Crabtree, R. H. *Organometallics* **1999**, 18, 1615. (b) Mazej, Z.; Borrmann, K. L.; Zemva, B. *Inorg. Chem.* **1998**, 37, 5912.
- (14) Richmond, T. G. *Coord. Chem. Rev.* **1990**, 105, 221.
- (15) Desiraju, G. R. *Angew. Chem., Int. Ed. Engl.* **1995**, 34, 2311.
- (16) Mareque Rivas, J. C.; Brammer, L. *Inorg. Chem.* **1998**, 37, 4756.
- (17) (a) Lewis, G. R.; Orpen, A. G. *Chem. Commun.* **1998**, 1873. (b) Gillon, A. L.; Orpen, A. G.; Starbuck, J.; Wang, X.-M.; Rodríguez-Martin, Y. Ruiz-Pérez, C. *Chem. Commun.* **1999**, 2287. (c) Gillon, A. L.; Lewis, G. R.; Orpen, A. G.; Rotter, S.; Starbuck, J.; Wang, X.-M.; Rodríguez-Martin, Y.; Ruiz-Pérez, C. *J. Chem. Soc., Dalton Trans.* **2000**, 3897. (d) Angeloni, A.; Orpen, A. G. *Chem. Commun.* **2001**, 343.
- (18) Desiraju, G. R.; Steiner, T. *The Weak Hydrogen Bond*; Oxford University Press: Oxford, U.K., 1999.
- (19) O'Hagan, D.; Rzepa, H. S. *Chem. Commun.* **1997**, 645.
- (20) Previous surveys of the geometry of hydrogen bonds involving halide ions have been reported,² as has a survey of C–H···Cl hydrogen bonds; see: Aakeröy, C. B.; Evans, T. A.; Seddon, K. R.; Pálinkó, I. *New J. Chem.* **1999**, 23, 145.
- (21) Allen, F. H.; Kennard, O. *Chem. Des. Automation News* **1993**, 8, 1, 31.
- (22) (a) C–H···Cl–C, *R* factor ≤ 0.070 and sigflag < 3; C–H···F–C *R* factor ≤ 0.060 and sigflag ≤ 3; C–H···Cl–M, *R* factor ≤ 0.040 and sigflag < 3. (b) Minimum distance cutoffs were also employed: H···F ≥ 1.6 Å, H···Cl ≥ 1.8 Å, H···Br ≥ 2.0 Å, and H···I ≥ 2.2 Å.
- (23) Bondi, A. J. *J. Chem. Phys.* **1964**, 68, 441.
- (24) Lommerse, J. P. M.; Stone, A. J.; Taylor, R.; Allen, F. H. *J. Am. Chem. Soc.* **1996**, 118, 3108.

- (25) Kroon, J.; Kanters, J. A. *Nature* **1974**, *248*, 667.
- (26) (a) GAMESS-UK is a package of ab initio programs written by: Guest, M. F.; van Lenthe, J. H.; Kendrick, J.; Schoffel, K.; Sherwood, P. with contributions from Amos, R. D.; Buenker, R. J.; van Dam, H. J.J.; Dupuis, M.; Handy, N. C.; Hillier, I. H.; Knowles, P. J.; Bonacic-Koutecky, V.; von Niessen, W.; Harrison, R. J.; Rendell, A. P.; Saunders, V. R.; Stone, A. J.; de Vries, A. H. The package is derived from the original GAMESS code of: Dupuis, M.; Spangler, D.; Wendoloski, J. NRCC Software Catalog, Vol. 1, Program No. QG01 (GAMESS), 1980. (b) Stevens, W. J.; Krauss, M.; Basch, H.; Jasien, P. G. *Can. J. Chem.* **1992**, *70*, 612. (c) Sadlej, A. J. *Theor. Chim. Acta* **1992**, *81*, 45 and references therein. (d) SBKJC VDZ ECP basis set: Stevens, W. J.; Krauss, M.; Basch, H.; Jasien, P. G. *Can. J. Chem.* **1992**, *70*, 612. (e) Ahlrichs DZP basis set: Schäfer, A.; Horn, H.; Ahlrichs, R. *J. Chem. Phys.* **1992**, *97*, 2571. (f) Stuttgart RLC ECP basis set: Bergner, A.; Dolg, M.; Kuechle, W.; Stoll, H.; Preuss, H. *Mol. Phys.* **1993**, *80*, 1431. (g) Basis sets were obtained from the Extensible Computational Chemistry Environment Basis Set Database, Version 1.0, as developed and distributed by the Molecular Science Computing Facility, Environmental and Molecular Sciences Laboratory, which is part of the Pacific Northwest Laboratory, P.O. Box 999, Richland, WA 99352, and funded by the U.S. Department of Energy. The Pacific Northwest Laboratory is a multiprogram laboratory operated by Battelle Memorial Institute for the U.S. Department of Energy under Contract DE-AC06-76RLO 1830. Contact David Feller, Karen Schuchardt, or Don Jones for further information.
- (27) Steiner, T.; Desiraju, G. R. *Chem. Commun.* **1998**, 891.
- (28) The large spike in the (O)H...I-M histogram at 165° corresponds to a single observation that lies in the range 160–170°. Since there are a total of only eight observations of O-H...X-M interactions, amplification of observations closer to 180° by the solid angle correction²⁵ assigns what is almost certainly an unrealistic importance to this single observation. To a lesser extent the same could be said of the smaller spike at 155° in the (O)H...Br-M histogram, since this is derived from only two observations.
- (29) (a) Arshadi, M.; Yamagni, R. Kebarle, P. *J. Phys. Chem.* **1970**, *74*, 1475. (b) Del Bene, J. E. *J. Phys. Chem.* **1988**, *92*, 2874. (c) Of course, the symmetric bifluoride ion, [F-H-F]⁻, exhibits an even stronger hydrogen bond, calculated at 39 kcal/mol: Gronert, S. *J. Am. Chem. Soc.* **1993**, *115*, 10258.
- (30) (a) The crystal structures from which the O-H...X-C geometries are taken have been examined carefully in an effort to identify the source of the apparently anomalous trends in geometries for the O-H...X-C interactions. In particular, the variation (and potential inaccuracy) of X-C bond lengths has been considered. While there are a small number of outliers compared with typical X-C distances,^{30b} removal of these structures has no effect on the trends in geometry already reported. (b) Allen, F. H.; Kennard, O.; Watson, D. G.; Brammer, L.; Orpen, A. G.; Taylor, R. *J. Chem. Soc., Perkin Trans. 2* **1987**, S1.
- (31) Peris, E.; Lee, J. C.; Rambo, J. R.; Eisenstein, O.; Crabtree, R. H. *J. Am. Chem. Soc.* **1995**, *117*, 3485.
- (32) In the present examination of these model systems, the geometries of the molecules were optimized in contrast to the prior preliminary report^{1b} in which idealized geometries were used. Optimized geometries are provided in the Supporting Information.
- (33) Examination of the variation of H...Cl-M angle with increasing coordination number at the metal suggests that there is a small steric effect on this angle arising from repulsions between ligands cis to the halide and the hydrogen bond donor group. This effect is anticipated to be greater for fluorine than for chlorine due to the shorter F-M and H...F distances involved, but appears to be insufficient to account for the differences in H...X-M angle observed between fluorine and the other halogens.
- (34) (a) Systematic geometric studies of C-H...O≡C-M and C-H...O=C-M₂ hydrogen bonds in organometallic carbonyl compounds do provide evidence for weak lone pair directionality at the carbonyl oxygen (i.e. acceptor anisotropy).^{34b,c} (b) Braga, D.; Biradha, K.; Grepioni, F.; Pedireddi, V. R.; Desiraju, G. R. *J. Am. Chem. Soc.* **1995**, *117*, 3156. (c) Braga, D.; Grepioni, F. *Acc. Chem. Res.* **1997**, *30*, 81.
- (35) (a) This failure of O-H...X-C interactions to follow anticipated trends in H...X-C angle is consistent with the anomalous behavior observed for H...X distance trends in O-H...X-C interactions (see prior discussion and footnote 30). (b) The two observations of N-H...I-C interactions exhibit H...I-C angles in the range 90–110°, while the four O-H...I-C interactions have angles of 80–120°.
- (36) The qualitative similarity between the potentials for CH₃X and *trans*-PdX(CH₃)(PH₃)₂ can be traced to a qualitative similarity between the orbital descriptions of M-X and C-X σ-bonds.
- (37) Landrum, G. A.; Goldberg, N.; Hoffmann, R. *J. Chem. Soc., Dalton Trans.* **1997**, 3605.
- (38) Horwitz, C. P.; Shriver, D. F. *Adv. Organomet. Chem.* **1984**, *23*, 219.
- (39) Wells, A. F. *Structural Inorganic Chemistry*, 5th ed.; Oxford University Press: Oxford, U.K., 1984.
- (40) Kulawiec, R. J.; Crabtree, R. H. *Coord. Chem. Rev.* **1990**, *99*, 89.
- (41) Plenio, H. *Chem. Rev.* **1997**, *97*, 3363.
- (42) Strauss, S. H. Personal communication.
- (43) Brammer, L. Unpublished work.
- (44) For an example of extensive C-H...F-B hydrogen bonding involving BF₄⁻ anions studied by neutron diffraction, see: Brammer, L.; Klooster, W.; Lemke, F. R. *Organometallics* **1996**, *15*, 1721.
- (45) For a discussion of charge-assisted C-H...F-P hydrogen bonding involving PF₆⁻ anions, see: Grepioni, F.; Cojazzi, G.; Draper, S. M.; Scully, N.; Braga, D. *Organometallics* **1998**, *17*, 296.
- (46) Reed, C. A. *Acc. Chem. Res.* **1998**, *31*, 133.
- (47) Strauss, S. H. *Chem. Rev.* **1993**, *93*, 927.
- (48) McBride, M. T.; Luo, T.-J. M.; Palmore, G. T. *Cryst. Growth Des.* **2001**, *1*, 39.
- (49) Davey, R. J.; Blagden, N.; Righini, S.; Alison, H.; Quayle, M. J.; Fuller, S. *Cryst. Growth Des.* **2001**, *1*, 59.
- (50) Thallypally, P. K.; Nangia, A. *CrystEngComm* **2001**, *27*.

CG015522K